ARMY RESEARCH LABORATORY

Solving Magnetic Diffusion Problems Using the PEEC Method

by Charles R. Hummer

ARL-TR-5165 **May 2010**

NOTICES

Disclaimers

The findings in this report are not to be construed as an official Department of the Army position unless so designated by other authorized documents.

Citation of manufacturer's or trade names does not constitute an official endorsement or approval of the use thereof.

Destroy this report when it is no longer needed. Do not return it to the originator.

Army Research Laboratory
Aberdeen Proving Ground, MD 21005-5069

ARL-TR-5165 **May 2010**

Solving Magnetic Diffusion Problems Using the PEEC Method

Charles R. Hummer
Weapons and Materials Research Directorate, ARL

REPORT DOCUMENTATION PAGE	Form Approved OMB No. 0704-0188

1. REPORT DATE *(DD-MM-YYYY)*	2. REPORT TYPE	3. DATES COVERED (From - To)
May 2010	Final	2008–2009

4. TITLE AND SUBTITLE
Solving Magnetic Diffusion Problems Using the PEEC Method

5a. CONTRACT NUMBER

5b. GRANT NUMBER

5c. PROGRAM ELEMENT NUMBER

6. AUTHOR(S)
Charles R. Hummer

5d. PROJECT NUMBER
AH43611102

5e. TASK NUMBER

5f. WORK UNIT NUMBER

7. PERFORMING ORGANIZATION NAME(S) AND ADDRESS(ES)
U.S. Army Research Laboratory
ATTN: RDRL-WMP-A
Aberdeen Proving Ground, MD 21005-5069

8. PERFORMING ORGANIZATION REPORT NUMBER
ARL-TR-5165

9. SPONSORING/MONITORING AGENCY NAME(S) AND ADDRESS(ES)

10. SPONSOR/MONITOR'S ACRONYM(S)

11. SPONSOR/MONITOR'S REPORT NUMBER(S)

12. DISTRIBUTION/AVAILABILITY STATEMENT
Approved for public release; distribution is unlimited.

13. SUPPLEMENTARY NOTES

14. ABSTRACT
In some electromagnetic problems, the paths of a current distribution in a conductor are known from the geometry or from the assumptions being used, but the magnitudes for each path are not known. The Partial Equivalent Electronic Circuit (PEEC) models the paths of the current distribution by wires carrying an unknown current. The current in each wire is found by assuming the wire forms an electrical circuit that has a resistance, a self inductance, a mutual inductance with the rest of the wires, and solving a matrix equation. Current distributions in the rails of a railgun and a copper cup are presented as examples of problems with linear and cylindrical geometries, respectively.

15. SUBJECT TERMS
magnetic, diffusion, railgun, rail, PEEC, Partial Equivalent Electronic Circuit

16. SECURITY CLASSIFICATION OF:			17. LIMITATION OF ABSTRACT	18. NUMBER OF PAGES	19a. NAME OF RESPONSIBLE PERSON
a. REPORT	b. ABSTRACT	c. THIS PAGE			Charles R. Hummer
Unclassified	Unclassified	Unclassified	UU	32	19b. TELEPHONE NUMBER (*Include area code*) 410-278-5680

Contents

List of Figures **iv**

List of Tables **v**

1. Introduction **1**

2. PEEC **2**

3. Railgun Rails **4**

3.1 Copper Rails 8

3.2 S0 Armature Rails 9

4. Copper Cup **12**

5. Conclusions **14**

6. References **15**

Appendix. Mutual and Self-Inductance Formulas **17**

Distribution List **22**

List of Figures

Figure 1. A current path through the elements for the rails. 6

Figure 2. Cladded rails for the S0 armature. 8

Figure 3. Rail current for the S0 armature. 10

Figure 4. Temperature distribution at 5 ms for solid copper, molybdenum cladding, and stainless steel cladding from left to right where the claddings are on the left side. 11

Figure 5. Current density distribution at 0.5 ms for solid copper, molybdenum cladding, and stainless steel cladding from left to right, where the claddings are on the left side. 11

Figure 6. Distribution of the magnitude of the diffused magnetic field into a copper cup, the cross section outlined in black, after 1.0 μs (left) and 5.0 μs (right) of the establishment of the 1.0 T magnetic field that is uniform in the positive z direction at large distances from the copper cup. 13

Figure A-1. Two elements with the locations of filaments (●) used for the mutual inductance in equation A-17. 20

List of Tables

Table 1. Material properties for copper 8
Table 2. Comparison of the inductance gradient at various times. 9
Table 3. Material properties of 304 stainless steel. 11
Table 4. Material properties of molybdenum. 11
Table 5. Inductance gradient for copper, molybdenum and 304 stainless steel cladding. 12
Table 6. Resistance gradient for copper, molybdenum and 304 stainless steel cladding. 12

INTENTIONALLY LEFT BLANK.

1. Introduction

In integrated circuits and other electronic devices, components may be connected together by long, straight conductors. The inductance and resistance of these conductors at various frequencies should be known to avoid unwanted signal loss, distortion or leakage to other conductors known as cross talk. An approach to calculate the frequency dependence on the inductance and resistance is based on the Partial Equivalent Electronic Circuit (PEEC) method (Ouda and Sebak, 1995) where a conductor is divided up into a number of elements. It is assumed that each of these elements has a uniform current density directed along its length. This is analogous to a number of insulated wires that are bundled into a cable. The cable is analogous to the conductor and the wires are analogous to the elements. Each wire or element is treated as a part of an equivalent electronic circuit with its own resistance, self inductance and a mutual inductance with every other wire. In some cylindrically symmetric problems where the current is azimuthally distributed, it is possible to divide up the conductors into a number of concentric rings each carrying a uniform current density. In this geometry, each ring or wire element is again treated as part of an equivalent electronic circuit with its own resistance, self inductance and mutual inductance with every other ring. Both cases give a matrix equation for a number of electronic circuits that are magnetically coupled together. In this report, PEEC is used to duplicate the calculations in a recent study in railguns (Powell and Zielinski, 2008), and used to find the temperature and current distribution in rails that have a cladding. As an example for applying PEEC to problems with cylindrical symmetry, the diffusion of a magnetic field into a cylindrically symmetric object is presented.

In a recent study of the temperature distribution, current distribution and the inductance of the rails in a railgun, Powell and Zielinski (2008) solved the coupled Maxwell and energy transport equations for infinitely long parallel rails having a width and a height, but no armature. Maxwell's equation was solved by calculating the magnetic vector potential inside the rails, between the rails and in the free space that extended out to a large distance as compared to the width, the height, and the spacing between the rails. Coupled with the Maxwell's equation were the equation for ohmic heating of the rails and the equation for heat conduction. Because the PEEC method uses the current density distribution in the rails as the basis for the solution of Maxwell's equation, calculations in the surrounding free space are avoided, which may ease some computational burden. The PEEC gave nearly identical results to Powell’s, even though heat conduction was not included. This method was again applied to rails that launched the S0 armature (Powell and Zielinski, 2005) having a mass of 2.0 kg to a velocity of 2.3 km/s. For a given current pulse, the current and temperature distributions were found when the rails were solid copper, cladded with 304 stainless steel and cladded with molybdenum. These calculations show that these claddings do reduce the surface temperature of the rails, but they do not explain

why the claddings fail to delay or prevent the formation of the plasma. The PEEC method, however, can easily provide the inductance gradient and resistance gradient of rails with novel geometries and composition, which are important parameters in designing railguns. To illustrate how to apply PEEC to problems with cylindrical symmetry, the diffusion of a magnetic field into a copper cup is solved. It is assumed that the magnetic field is uniform at distances far from the copper cylinder, parallel to the cylinder's central axis, and it is applied instantaneously.

2. PEEC

The derivation of the matrix equation for the PEEC starts with Faraday's law for stationary conductors in the form

$$\vec{E}(\vec{r},t) = -\nabla\varphi - \frac{\partial\vec{A}(\vec{r},t)}{\partial t} \ , \tag{1}$$

where $\vec{E}$, φ, and $\vec{A}$ are the electric field vector, the electric potential, and the magnetic field vector potential, respectively (Corson and Lorrain, 1962).

Using Ohm's law,

$$\vec{J}(\vec{r},t) = \sigma(\vec{r},t)\,\vec{E}(\vec{r},t) \ , \tag{2}$$

and the magnetic vector potential for a current density distribution $\vec{J}(\vec{r},t)$ when the displacement current is ignored,

$$\vec{A}(\vec{r},t) = \frac{\mu_o}{4\pi}\int d\tau' \frac{\vec{J}(\vec{r}',t)}{\left|\vec{r}-\vec{r}'\right|} \ , \tag{3}$$

Faraday's law becomes

$$\frac{\vec{J}(\vec{r},t)}{\sigma(\vec{r},t)} = -\nabla\varphi - \frac{\mu_o}{4\pi}\frac{\partial}{\partial t}\int d\tau' \frac{\vec{J}(\vec{r}',t)}{\left|\vec{r}-\vec{r}'\right|} \ , \tag{4}$$

where $\sigma(\vec{r},t)$ in equation 2 is the distribution of the electrical conductivity.

When the conductor is divided up into a number of elements, *n* in equation 5, the integral in equation 3 may then be expressed as a sum of integrals that are performed over each element. Let all of these elements have equal length *l* and be parallel to the z-axis so that the current density and the magnetic vector potential have only the z component, and the gradient of φ becomes $\partial\varphi/\partial$z. This is assuming that this common length is much larger than the cross sectional

dimensions of the conductor. Thus the vector notation for these quantities will be dropped with the understanding that *A* and *J* are the z component of a vector. With this understanding and assuming a uniform current distribution for each element varies with time, equation 3 may then be approximated by

$$A(\vec{r},t) = \frac{\mu_o}{4\pi}\sum_{i=1}^{n} J_i(t)\int d\tau_i' \frac{1}{\left|\vec{r}-\vec{r}_i'\right|} \ , \tag{5}$$

where $\vec{r}_i'$ is a location of a point inside the i*th* element and $d\tau_i'$ is the unit volume within the element. J_i is the assumed uniform current density for the element. Using equation 5 instead of equation 3 and integrating over the volume of the j*th* element when it has a uniform conductivity σ_j gives

$$\frac{J_j\, a_j\, l}{\sigma_j} = -\Delta\varphi_j\, a_j - \frac{\mu_o}{4\pi}\frac{\partial}{\partial t}\sum_{i=1}^{n} J_i(t)\int d\tau_j' \int\ d\tau_i' \frac{1}{\left|\vec{r}_j'-\vec{r}_i'\right|} \ , \tag{6}$$

where a_j is the cross sectional area of the j*th* element and $\Delta\varphi$ is the potential difference between the ends of the element. The integrals in equation 6 are the magnetic coupling between elements *i* and *j* which is related to the mutual inductance between them. By convention, this mutual inductance that depends only on the geometry of the conductors for this application is

$$M_{i,j} = \frac{\mu_o}{4\pi\, a_i\, a_j}\int d\tau_j' \int d\tau_i' \frac{1}{\left|\vec{r}_j'-\vec{r}_i'\right|} \ . \tag{7}$$

Tables and formulas for $M_{i,j}$ have been presented for a large number of different geometries and configurations of conductors by Grover (1946) as an example of a large body of literature. Solving equation 7 for the integrals and substituting the result into equation 6 yields

$$\frac{J_j(t)\, a_j\, l}{\sigma_j} = -\Delta\varphi_j\, a_j - a_j\frac{\partial}{\partial t}\sum_{i=1}^{n} J_i(t)\, a_i\, M_{i,j} \ , \tag{8}$$

or, in other terms,

$$I_j(t)R_j = -\Delta\varphi_j - \sum_{i=1}^{n}\frac{dI_i(t)}{dt}\, M_{i,j} \ , \tag{9}$$

where $I_j = J_j\, a_j$ is the current and $R_j = l/(\sigma_j\, a_j)$ is the resistance for the element. It will be shown later, however, that this resistance is $R_j = 2l/(\sigma_j\, a_j)$ for parallel rails.

This matrix equation is a commonly accepted circuit equation for a number of electronic circuits that are magnetically coupled. Each circuit has a resistance R_j, a voltage $\Delta\varphi_j$, and a self inductance $M_{j,j}$: the matrix element on the diagonal. Each circuit is coupled to the other circuits by the off-diagonal matrix elements $M_{i,j}$, *i* and *j* are not equal, which are the mutual inductances.

It is commonly assumed in PEEC literature that the current in the elements and the voltage are harmonically oscillating at a constant angular frequency ω. By letting $I_j(t) = I_j \exp(-i\omega t)$ and $\Delta\varphi = \Delta\varphi \exp(-i\omega t)$, equation 9 becomes an algebraic equation that is independent of time but dependent on ω. These assumptions are not taken here, because the currents in the elements are not harmonically oscillating.

In some cases, if a total current in the circuits can be defined, a total inductance of the circuits can be found from the total energy of the magnetic field, E_m in equation 20, which is defined as

$$E_m(t) = \frac{1}{2}\sum_{i=1,\, j=1}^{n} I_i(t) M_{i,j}\, I_j(t) = \frac{L(t)\ \ \mathrm{I}^2(t)}{2} \ . \tag{10}$$

This energy is then equated to the energy stored in an equivalent total inductor having an inductance L and a total current I*(t)*. In the case for the rails, the total current to the rails is known, and, thus, the inductance gradient of the rails can be calculated for rails with an assumed length.

Excluding heat conduction, the increase in temperature of the elements is found by equating the ohmic heating over some time interval *dt* (the left side of equation 11) to the heat of the element (the right side of equation 11):

$$\frac{l\, I_i^2(t)}{\sigma(T_i)\, a_i}\, dt = \rho\, l\, a_i\, C_p(T_i)\, dT_i \ . \tag{11}$$

In this equation, l is the length and a_i is the cross sectional area of the element having a density ρ. When the electrical conductivity $\sigma(T)$ and the heat capacity $C_p(T)$ depend on the temperature T, the rate of temperature increase for an element is

$$\frac{dT_i}{dt} = \frac{I_i^2(t)}{\rho\, a_i^2 \sigma(T_i)\, C_p(T_i)} \ . \tag{12}$$

3. Railgun Rails

Equation 9 must be modified, however, for the constraints imposed by a railgun problem before solving it for the time derivative of the currents. One constraint is that the voltage across all the elements are equal. The other constraint is that the total current for all the elements is given. In preparation for imposing these constraints, equation 9 is parsed into two equations. The equation for $j \le n-1$ is written as

$$I_j(t)R_j = -\Delta\varphi_j - M_{n,j}\frac{dI_n(t)}{dt} - \sum_{i=1}^{n-1}\frac{dI_i(t)}{dt}M_{i,j} \ . \tag{13}$$

Another equation for $j = n$ is

$$I_n(t)R_n = -\Delta\varphi_n - M_{n,n}\frac{dI_n(t)}{dt} - \sum_{i=1}^{n-1}\frac{dI_i(t)}{dt}M_{i,n} \ . \tag{14}$$

Since the total current is the sum of all the currents of the elements, one of these currents is no longer independent. Arbitrarily choose $I_n(t)$ as the dependent current that is given by

$$I_n(t) = \mathrm{I}(t) - \sum_{i=1}^{n-1} I_i(t) \ . \tag{15}$$

Substituting the time derivative of this equation into equation 13 gives

$$I_j(t)R_j = -\Delta\varphi_j - M_{n,j}\frac{d\mathrm{I}(t)}{dt} - \sum_{i=1}^{n-1}\frac{dI_i(t)}{dt}(M_{i,j} - M_{n,j}) \ , \tag{16}$$

and equation 14 becomes

$$I_n(t)R_n = -\Delta\varphi_n - M_{n,n}\frac{d\mathrm{I}(t)}{dt} - \sum_{i=1}^{n-1}\frac{dI_i(t)}{dt}(M_{i,n} - M_{n,n}) \ . \tag{17}$$

Equation 15 was not substituted into the left-hand side of equation 14 because $I_n(t)$ is known at this time. If the voltages across all the elements are equal, then the voltages can be eliminated by subtracting equation 17 from equation 16:

$$I_j(t)R_j - I_n(t)R_n = (M_{n,n} - M_{n,j})\frac{d\mathrm{I}(t)}{dt} - \sum_{i=1}^{n-1}\frac{dI_i(t)}{dt}(M_{i,j} - M_{n,j} - M_{i,n} + M_{n,n}) \ . \tag{18}$$

After defining a new matrix $Z_{i,j} = M_{i,j} - M_{n,j} - M_{i,n} + M_{n,n}$ and finding its inverse $Z^{-1}_{i,j}$, the time derivatives for the first n-1 elements are

$$\frac{dI_i(t)}{dt} = \sum_{j=1}^{n-1} Z^{-1}_{i,j}\left(I_n(t)R_n - I_j(t)R_j + (M_{n,n} - M_{n,j})\frac{d\mathrm{I}}{dt}\right) \ . \tag{19}$$

The time derivative for the nth element can now be determined simply by adding all the time derivatives of the first n-1 elements and subtracting the sum from the time derivative of the total current:

$$\frac{dI_n(t)}{dt} = \frac{d\mathrm{I}}{dt} - \sum_{i=1}^{n-1}\frac{dI_i(t)}{dt} \ . \tag{20}$$

Thus, the time derivatives for all the currents are now determined at the given time.

The construction of the inductance matrix $M_{i,j}$ elements in equation 9 uses two fundamental equations that are presented in the appendix. One fundamental equation is for the self inductance of a long rectangular bar $S(w,h,l)$, where w is the width, h is the height and l is the length of the bar. The other fundamental equation is for the mutual inductance of element "a" with respect to element "b" $M(w_a, h_a, x_a, y_a, w_b, h_b, x_b, y_b, l)$ both having equal lengths l. w_a and h_a are the width and height respectively of element "a" with its center located at (x_a, y_a). w_b and h_b are the width and height respectively of element "b" with its center located at (x_b, y_b). This mutual inductance is independent from the origin of the coordinates for (x_a, y_a) and (x_b, y_b). The origin in figure 1, however, is assumed to be located half way between the two inner surface of the rails, so that the y-z plane and the x-z plane are planes of symmetry of the rails. Although the rail symmetry about the x-z plane could be included to reduce the number of elements, this symmetry is ignored here.

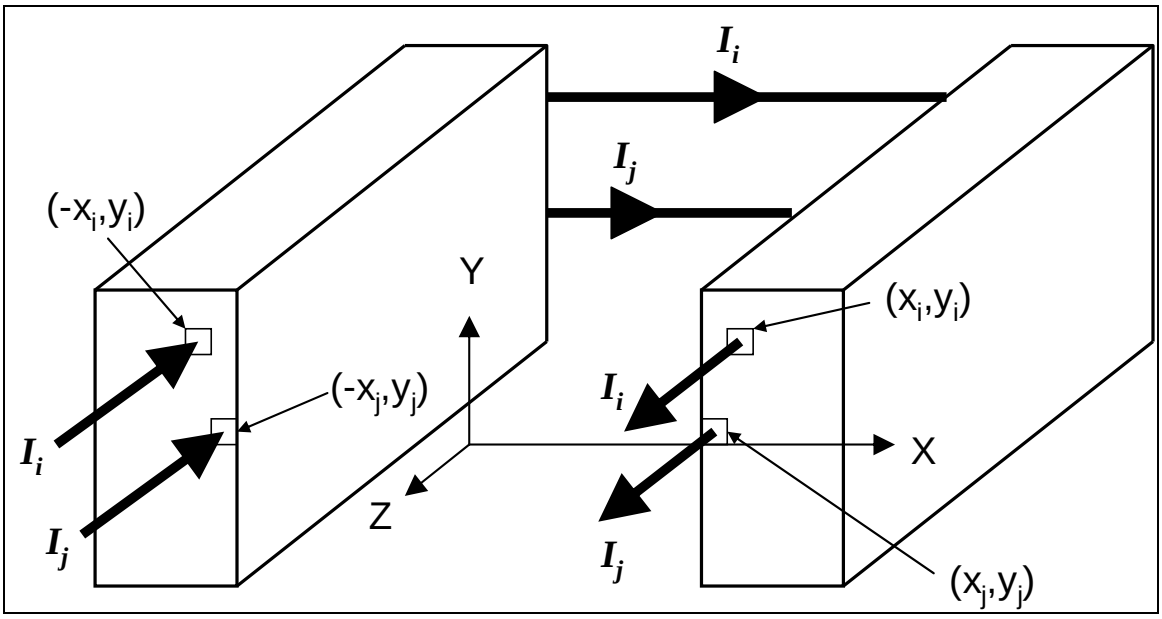

Figure 1. A current path through the elements for the rails.

Let the position of the ith element be located at (x_i, y_i) and carrying a current I_i in the positive z-direction. The element that is carrying the equal but opposite current $-I_i$ is located at $(-x_i, y_i)$, provided that both elements have equal widths w_i and equal heights h_i, figure 1. The magnetic fields from the currents crossing over from one rail to the next that represent the current through the armature, can be ignored for rails having a length much larger than the spacing between them.

By symmetry, there is an element located at $(x_i, -y_i)$ that is carrying an equal current I_i to the one at (x_i, y_i) and there is another element located at $(-x_i, -y_i)$ that is carrying the equal but opposite current $-I_i$ to the one at that (x_i, y_i), provided that these latter two elements, $(x_i, -y_i)$ and $(-x_i, -y_i)$, also have equal widths and equal heights to the one at (x_i, y_i). As stated before, this symmetry is not used here. Thus the current in the element at (x_i, y_i) is not assumed to be equal to the element $(x_i, -y_i)$, but taken to be an independent variable. The elements at (x_i, y_i) and $(-x_i, y_i)$, as shown in Figure 1 constitute a circuit that has an inductance and a resistance. The inductance of this circuit is the sum of the self inductances for each element that are equal, the mutual inductance of the element at (x_i, y_i) with respect to the element at $(-x_i, y_i)$, and the mutual inductance of the element at $(-x_i, y_i)$ with respect to the element at (x_i, y_i):

$$M_{i,i} = 2\, S(w_i,h_i,l) - M(w_i, h_i, x_i, y_i, w_i, h_i, -x_i, y_i,l) - M(w_i, h_i, -x_i, y_i, w_i, h_i, x_i, y_i, l)\ . \quad (21)$$

Because $M(w_i, h_i, x_i, y_i, w_i, h_i, -x_i, y_i,l) = M(w_i, h_i, -x_i, y_i, w_i, h_i, x_i, y_i, l)$, the diagonal elements of the inductance matrix are

$$M_{i,i} = 2\ (\ S(w_i,h_i,l) - M(w_i, h_i, x_i, y_i, w_i, h_i, -x_i, y_i,l)\ )\ . \quad (22)$$

The minus sign in front of the mutual inductance function comes from the currents being equal but having opposite directions. If the current in both of these elements were in the same direction, such as the positive z-direction, then there would have been a positive sign. The total resistance for this circuit is $R_i = 2\, l/(w_i\, h_i\, \sigma_i)$, because the current path length is twice the rail length.

The off-diagonal elements of the inductance matrix are the mutual inductances of the *i*th rail element and its complement in the negative x-direction with respect to the *j*th rail element and its complement in the negative x-direction as shown in figure 1, which is $M_{i,j} = M(w_i, h_i, x_i, y_i, w_j, h_j, x_j, y_j,l) - M(w_i, h_i, x_i, y_i, w_j, h_j, -x_j, y_j,l) + M(w_i, h_i, -x_i, y_i, w_j, h_j, -x_j, y_j,l) - M(w_i, h_i, -x_i, y_i, w_j, h_j, x_j, y_j,l)$. However, the mutual inductance between the *i*th and the *j*th elements on the positive side of the x-axis is equal to the mutual inductance between the *i*th and the *j*th elements on the negative side of the x-axis; $M(w_i, h_i, x_i, y_i, w_j, h_j, x_j, y_j,l) = M(w_i, h_i, -x_i, y_i, w_j, h_j, -x_j, y_j,l)$. Note that their mutual inductances are positive because the current in these two pairs are in the same direction. Also, the mutual inductance between the *i*th element on the positive side of the x-axis and the *j*th element on the negative side of the x-axis is the same as the mutual inductance between the jth element on the positive side of the x-axis and the *i*th element on the negative side of the x-axis; $M(w_i, h_i, x_i, y_i, w_j, h_j, -x_j, y_j,l) = M(w_i, h_i, -x_i, y_i, w_j, h_j, x_j, y_j,l)$. The signs for these terms are negative because the current in these pairs of bars are equal but opposite. Thus the off-diagonal elements of the inductance matrix are

$$M_{i,j} = 2\ (\ M(w_i, h_i, x_i, y_i, w_j, h_j, x_j, y_j,l) - M(w_i, h_i, x_i, y_i, w_j, h_j, -x_j, y_j,l)\ )\ . \quad (23)$$

3.1 Copper Rails

PEEC will now be applied to the identical problem recently reported by Powell and Zielinski (2008), where each copper rail has a width w = 19.4 mm, a height h = 34 mm and a spacing s = 44 mm between them. See figure 2 as an illustration of w, h and s for another set of rails having different dimensions. The material properties for copper are shown in table 1. And the current in this case is

$$I(t) = 5.0 \times 10^5 \tanh(t / 1.0 \times 10^{-4}) \ , \tag{24}$$

where t is in seconds and the current is in amps. Although the symmetry above and below the x-axis was ignored, the resulting current and temperature distributions did have the correct symmetry. Using the symmetry, this calculation was repeated with half the number of elements and gave identical results.

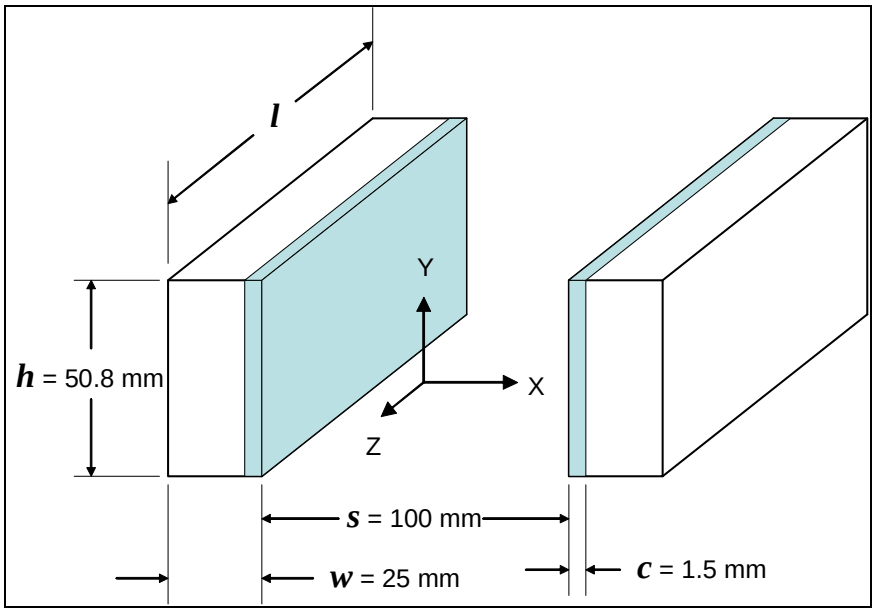

Figure 2. Cladded rails for the S0 armature.

Table 1. Material properties for copper.

Property	Value
Heat capacity (J/kg/K)	$C_p(T) = 360.0 + 0.1\ T$
Resistivity (Ω m)	$1/\sigma(T) = -5.42 \times 10^{-9} + 7.81 \times 10^{-11}\ T$
Density (kg/m^3)	$\rho = 8900.0$

The current density distribution and the temperature distribution of these calculations agree very well with the distributions given by Powell and Zielinski (2008). As an indication of the agreement, the inductance gradients are compared in table 2 at various times.

Table 2. Comparison of the inductance gradient at various times.

t (μs)	**Powell *L′* (μH/m)**	**Present *L′* (μH/m)**
200	0.591	0.567
500	0.598	0.590
1000	0.615	0.613
1500	0.627	0.627
5000	0.650	0.656

At the very early times, all the current should be distributed on the outside surfaces of the rails and no current inside the rails. By assuming an infinite conductivity for the rails, Kerrisk (1982) gave empirical formulas that were based on more detailed calculations for the inductance gradient for these surface current distributions. These formulas gave an inductance gradient to be 0.56 μH/m for these rails, which compares well with the present calculation at 200 μs. Powell speculated that his inductance at this time was high, because his model may not have had adequate resolution for the current distribution near the corners. Thus it seems that the present approach has a better resolution for the current distribution at these early times. At later times when the current distribution has diffused into the rails, both calculations give virtually identical inductance gradients. At the latest time, 5000 μs, the current distribution is almost uniform. If the current distribution was uniform, the inductance gradient according to Grover (1946) would be 0.67 μH/m (see equation A-15 in the appendix). It is not expected that the inductance gradient of the present calculation should approach this value exactly at a later time, because the rails do not have a uniform conductivity due to a non-uniform temperature distribution.

3.2 S0 Armature Rails

In a previous study (Powell and Zielinski, 2005), a two-dimensional (2-D) model was used to investigate the current and temperature distributions in the rails and an armature, designated as the “S0 armature,” of a rail gun. Assuming a rail current that is typically used at a pulse power facility in Kirkcudbright, Scotland (Hammon et al., 1993), the conditions for a contact transition, the formation of a plasma gap between the rail and the armature, were investigated. When this occurs, the rails and the armature are damaged, and the performance is also adversely affected. It was speculated that a metal cladding starting at the exit end of the rails and extending to some distance into the bore could prevent this transition. This study considered rails with no cladding and then considered rails that had a stainless steel cladding. It was concluded that the cladding did not prevent contact transition (Powell and Zielinski, 2008).

Since this cladding does not extend from end to end, PEEC cannot be used. It will be assumed, however, that the cladding does extend over the entire length of the rails as shown in figure 2, which also shows the dimensions of the rails and the cladding.

As shown in figure 3, the total current I (in amps) as a function of time t (in seconds) of the rails used for both cases is taken to be

$$I(t) = 1.933\times10^{6}\sin(981.75t) \text{ for } 0 \le t \le 1.6\times10^{-3}\ , \tag{25}$$

$$I(t) = 1.933\times10^{6} \text{ for } 1.6\times10^{-3} < t \le 3.3\times10^{-3}\ , \tag{26}$$

and

$$I(t) = 1.933\times10^{6}(1 - 2.558\times10^{5}\,\Delta t^{2} + 7.6\times10^{7}\,\Delta t^{3}) \text{ for } 3.3\times10^{-3} < t \le 5.0\times10^{-3}\,, \tag{27}$$

where $\Delta t = t - 3.3\times10^{-3}$. This equation, however, does not follow some of the small variations in current form that was used in the previous study (Powell et al., 2005; Hammon et al., 2003).

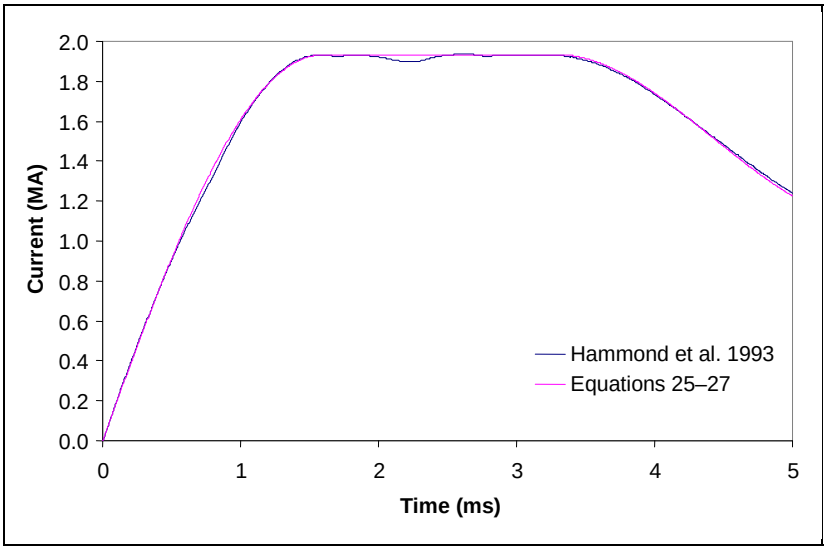

Figure 3. Rail current for the S0 armature.

Using the thermodynamic properties for 304 stainless steel given in table 3, the thermodynamic properties for molybdenum given in table 4, and the current pulse, the final temperature distribution of the rails were calculated at 5 ms, figure 4, when the temperatures should be the largest. The current distributions were also calculated at 0.5 ms, figure 5, when the current densities should be large. The left edges in figure 4 and figure 5 are the inside surface of the right rail in figure 2 and the bottom edges in figures 4 and 5 are the midline of the right rail in figure 2. The inductance gradient and the resistance gradient for these rails are listed at various times in tables 5 and 6, respectively.

Table 3. Material properties of 304 stainless steel.

Property	Value
Heat capacity (J/kg/K)	$C_p(T(K)) = 500.0$
Resistivity (Ω m)	$1/\sigma(T(K)) = 5.17 \times 10^{-7} + 6.90 \times 10^{-10}$ T
Density (kg/m^3)	$\rho = 8030.0$

Table 4. Material properties of molybdenum.

Property	Value
Heat capacity (J/kg/K)	$C_p(T(K)) = 220.7 + 0.1$ T
Resistivity (Ω m)	$1/\sigma(T(K)) = -2.82 \times 10^{-8} + 2.73 \times 10^{-10}$ T
Density (kg/m^3)	$\rho = 10220.0$

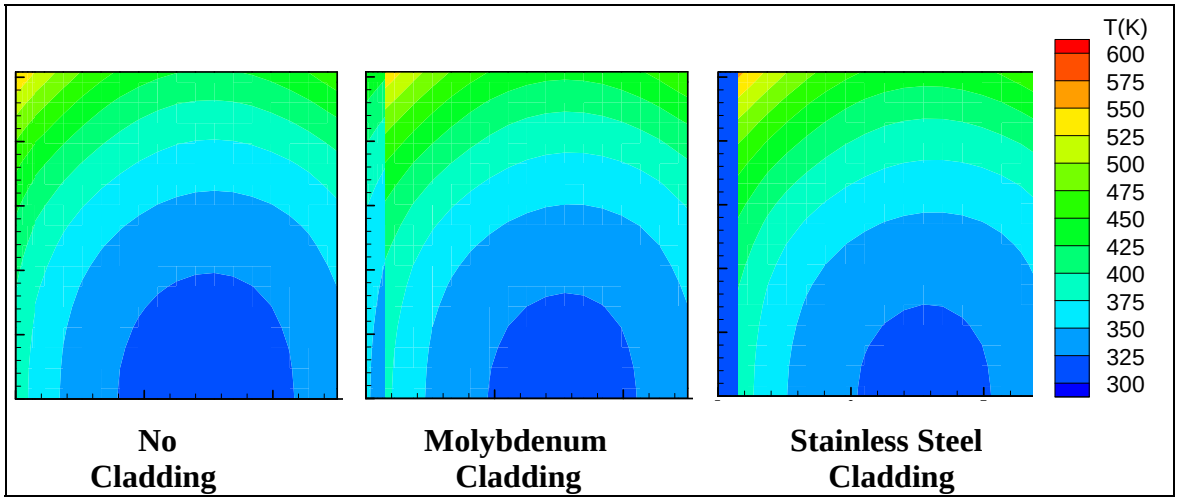

Figure 4. Temperature distribution at 5 ms for solid copper, molybdenum cladding, and stainless steel cladding from left to right where the claddings are on the left side.

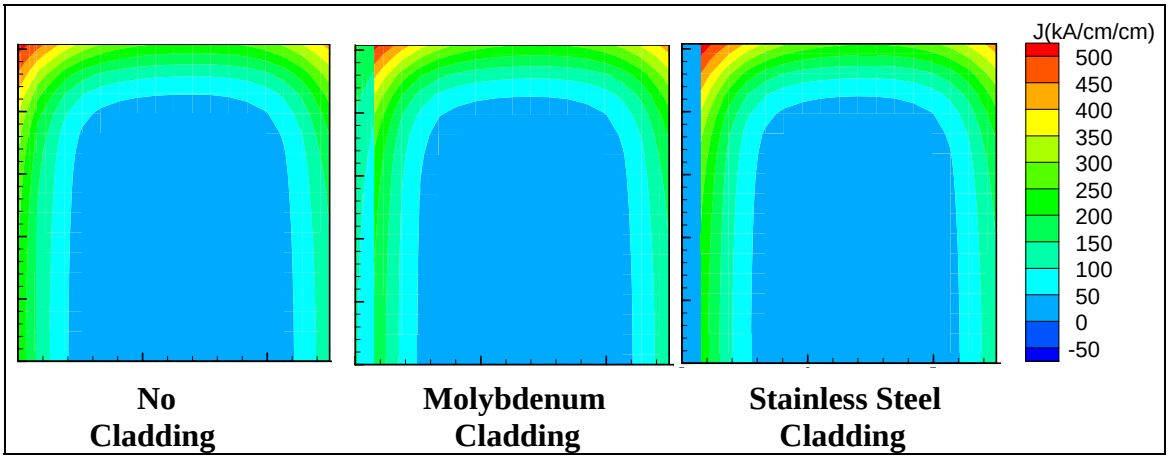

Figure 5. Current density distribution at 0.5 ms for solid copper, molybdenum cladding, and stainless steel cladding from left to right, where the claddings are on the left side.

Table 5. Inductance gradient for copper, molybdenum, and 304 stainless steel cladding.

Time (ms)	Copper (μH/m)	Molybdenum (μH/m)	304 S. S. (μH/m)
0.5	0.680	0.688	0.694
1.0	0.693	0.701	0.707
2.0	0.723	0.732	0.738
3.0	0.743	0.752	0.757
4.0	0.768	0.777	0.782
5.0	0.817	0.825	0.830

Table 6. Resistance gradient for copper, molybdenum, and 304 stainless steel cladding.

Time (ms)	Copper (μΩ/m)	Molybdenum (μΩ/m)	304 S. S. (μΩ/m)
0.5	28.5	29.7	30.3
1.0	29.2	30.4	31.1
2.0	31.1	32.5	33.3
3.0	32.8	34.4	35.3
4.0	34.5	36.3	37.4
5.0	35.7	37.7	38.8

The temperature distributions in all cases have a maximum at the corners near the gap of the copper. Although not obvious in figure 4, the maximum temperature is at the upper left corner of the copper rail when it has the stainless steel cladding is greater than the bare copper rail and the one with the molybdenum cladding. Thus, a cladding may increase the temperature of the copper, and the cladding can reduce the temperature of the inside surface. Therefore, the higher resistivity of the stainless steel relative to the molybdenum diverts more current into the copper to produce a higher temperature in the copper.

4. Copper Cup

As an example for using PEEC for a problem having cylindrical symmetry, let a uniform magnetic field at a large distances be suddenly applied to a copper cup as shown in figure 6. The tubular part of the copper cup has an outside radius of 0.015 m and a total outside length of 0.025 m, with a 0.005-m-thick wall. The bottom of the cup at z = 0.0 m is also 0.005 m thick. Heating of the copper is ignored. After the cup is divided up into rings with a square cross section, the induction matrix $M_{i,j}$ in equation 9 is calculated by the formulas for the self-inductance and the mutual inductance given in the appendix. Since each ring does not have an applied potential $\Delta\varphi_j = 0$. Thus, from equation 9, the time derivative of the current in each ring is

$$\frac{dI_i(t)}{dt} = -\sum_{j=1}^{n} M_{i,j}^{-1} \; I_j(t) R_j \;\; , \tag{28}$$

where R_j is the resistance of the jth ring. To begin the solution, the current at zero time must be established. Before the magnetic field is applied, there is zero magnetic flux through the rings. Just after the magnetic field is applied, the total magnetic flux through each ring, the sum of the applied magnetic flux, the magnetic flux of the ring itself, and the magnetic fluxes from all the other rings, is 0:

$$0 = \Psi_i + \sum_{j=1}^{n} M_{i,j} I_j(0) \;\; , \tag{29}$$

where $\Psi_i = B\pi r_i^2$. B is the magnitude of the applied magnetic field (1.0 T) and r_i is the radius of the ith ring. After solving equation 29 for the currents at time zero, currents at later times were numerically found by using the 4th order Runge-Kutta method. Using these currents and the applied magnetic field, the magnetic field can be calculated anywhere near the cup, by adding the applied magnetic field and the magnetic fields produced by the rings that has the calculated current $I_j(t)$. The distribution of the magnitude of the magnetic field 5.0 and 10.0 μs after the external magnetic field began are shown in figure 6. As expected, the magnetic field is larger at some distance from the outer wall of the cup. The eddy currents in the cup produce a magnetic field in the opposite direction of the applied magnetic field within the cup, but the magnetic field of these eddy currents bend around into the same direction as the applied magnetic field outside the cup.

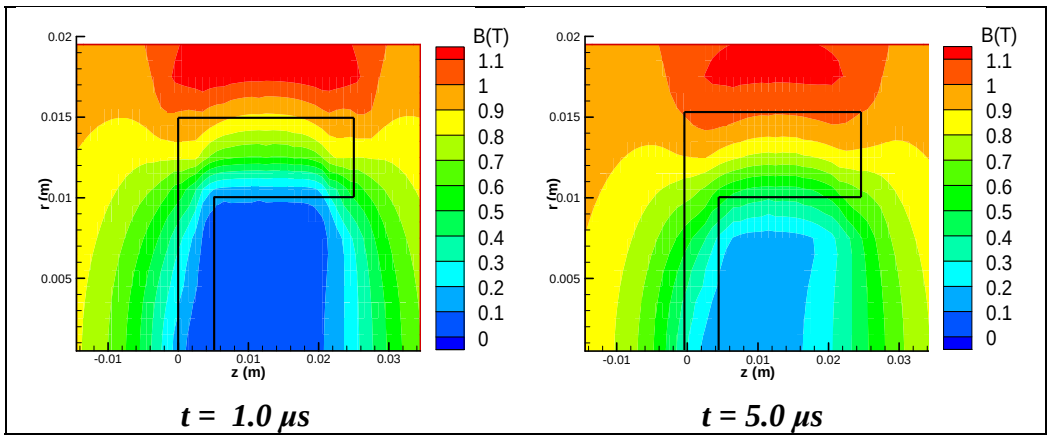

Figure 6. Distribution of the magnitude of the diffused magnetic field into a copper cup, the cross section outlined in black, after 1.0 μs (left) and 5.0 μs (right) of the establishment of the 1.0 T magnetic field that is uniform in the positive z direction at large distances from the copper cup.

5. Conclusions

It has been demonstrated that the PEEC method can be applied to a number of different kinds of magnetic field problems, such as the cladding of the rails in railguns. The purpose of cladding the rails is to delay the transition of the armature as it is nearing the muzzle of the electromagnetic gun by preventing the sliding surfaces of the rails from becoming too hot. These calculations indicate that the cladding should prevent this heating as shown in figure 4. Indeed, stainless steel should be more effective than molybdenum even though stainless steel is more resistive than molybdenum. A 2-D calculation (Powell and Zielinski, 2005) of the temperature and current distribution of the armature and the stainless steel cladded rails, however, showed that the armature still had a higher temperature than when the rails were solid copper. The current distribution given by the PEEC method, however, could be used as a boundary condition for the more detailed calculations, and it can easily estimate the inductance gradient and the resistance gradient of a railgun design.

The PEEC method is now being applied to other problems, such as the launching of metal plates by a magnetic field. In addition, this method can be modified to account for the linear magnetic properties of materials (Antonini et al., 2006; Keradec et al., 2005).

6. References

Antonini, G.; Sabatini, M.; Miscione, G. PEEC Modeling of Linear Magnetic Materials. *IEEE International Symposium on Electromagnetic Compatibility*, 14–18 August 2006; Vol. 1: pp 93–98.

Corson, D.; Lorrain, P. *Introduction to Electromagnetic Fields and Waves*; Freeman, W. H., Ed.; San Francisco, CA, 1962.

Grover, F. W. *Inductance Calculations Working Formulas and Tables*; Dover Publications: New York, 1946.

Hammon, H. G.; Dempsey, J.; Strachan, D.; Raos, R.; Haugh, D.; Whitby, F. P.; Holland, M. M.; Eggers, P. The Kirkcudbright Electromagnetic Launch Facility. *IEEE Transactions on Magnetics* **1993**, *29*, 975.

Keradec, J-P.; Clavel, E.; Gonnet, J-P.; Mazauric, V. Introducing Linear Magnetic Materials in PEEC Simulations. Principles, Academic and Industrial Applications. *Industry Applications Conference, 2005 Fourtieth IAS Annual Meeting*, 2–6 October 2005; Vol. 3: pp 2236–2240.

Kerrisk, J. F. *Current Diffusion in Rail-Gun Conductors*; LA-9401-MS; Los Alamos National Laboratory: Los Alamos, NM, 1982.

Ouda, M.; Sebak, A. Efficient Method of Frequency Dependent Inductance and Resistance Calculations. *WESCANEX 95, Communications, Power and Computing, Conference Proceedings, IEEE.*, Vol. 2: 1995; p 473.

Powell, J. D.; Zielinski, A. E. *Electrodynamics of the Rail-Armature Interface in a Solid-Armature Railgun*; ARL-TR-3663; U.S. Army Research Laboratory: Aberdeen Proving Ground, MD, 2005.

Powell J. D.; Zielinski A. E. *Two-Dimensional Current Diffusion in the Rails of a Railgun*; ARL-TR-4618; U.S. Army Research Laboratory: Aberdeen Proving Ground, MD, 2008.

INTENTIONALLY LEFT BLANK.

Appendix. Mutual and Self-Inductance Formulas

The calculation of the inductance matrix $M_{i,j}$ is based on two fundamental equations. One fundamental equation is the self inductance of a long rectangular bar *S(w,h,l),* and the other fundamental equation is the mutual inductance between two long rectangular bars of equal length *M(w_a, h_a, x_a, y_a, w_b, h_b, x_b, y_b, l).* These two fundamental equations are found by first performing the general integral in equation 7 over the *z* and *z'* coordinates for a pair of filaments of equal length *l* that are parallel with the z-axis and having arbitrary cross sections:

$$M = \frac{\mu_o l}{2\pi\, a\, a'} \int dx\, dy\, dx'\, dy' \left(\ln\left(\frac{l}{s} + \sqrt{1 + \frac{l^2}{s^2}} \right) - \sqrt{1 + \frac{s^2}{l^2}} + \frac{s}{l} \right), \tag{A-1}$$

where $s^2 = (x - x')^2 + (y - y')^2$, the cross sectional area for the primed and unprimed *i*th and the *j*th elements are a_i and a_j, respectively. If the primed x and y coordinates are of a point in the cross section of one conductor and the unprimed x and y coordinates are for a point in the cross section of a separate conductor, then *M* would be the mutual inductance between the two conductors. If the prime and unprimed x-y coordinates are for two points in the cross section of a single conductor, the *M* would give the self inductance of the single conductor. Grover[1] assumes that the length of the conductors are much larger than the dimensions of the cross sections. Thus, this integral is approximated by

$$M = \frac{\mu_o l}{2\pi\, a\, a'} \int dx\, dy\, dx'\, dy' \left(\ln\left(\frac{2l}{s} \right) - 1 \right), \tag{A-2}$$

or

$$M = \frac{\mu_o\, l\, (\ln(2l) - 1)}{2\pi} - \frac{\mu_o\, l}{4\pi\, a\, a'} \int dx\, dy\, dx'\, dy'\ \ln\left((x - x')^2 + (y - y')^2 \right). \tag{A-3}$$

The integral in this equation is defined as the geometric mean distance (GMD) by Grover or simply R, which is

$$\ln(R) = \frac{1}{2\, a\, a'} \int dx\, dy\, dx'\, dy'\ \ln\left((x - x')^2 + (y - y')^2 \right), \tag{A-4}$$

so that

$$M = \frac{\mu_o\, l}{2\pi} \left(\ln\left(\frac{2l}{R} \right) - 1 \right). \tag{A-5}$$

[1] Grover, F. W. *Inductance Calculations Working Formulas and Tables*; Dover Publications: New York, 1946.

Because the analytic expression for some of cross sectional areas are complicated, Grover presented their values in tables and graphs for various cross sections, which served the purpose at that time. Today, however, it is preferable to use analytic expressions that are presented here for some cases.

The diagonal elements of the inductance matrix are the self inductance of the elements having a rectangular cross section. Let the width and height of the rectangle be *w* and *h*, respectively. The GMD for a rectangular bar is

$$\ln(R) = \frac{1}{2w^2h^2}\int_{-w/2}^{w/2} dx \int_{-w/2}^{w/2} dx' \int_{-h/2}^{h/2} dy' \int_{-h/2}^{h/2} dy_j \ln\left((x-x')^2 + (y-y')^2\right) . \tag{A-6}$$

After performing the integrals, the GMD is

$$\ln(R) = \ln(w+h) - 1.5 + \ln(e(\alpha)) \ , \tag{A-7}$$

where

$$\begin{aligned} ln(e(\alpha)) = {} & \frac{ln(\alpha)}{12}\left(\alpha^2 - \alpha^{-2}\right) - ln(\alpha^{0.5} + \alpha^{-0.5}) \\ & - ln(\alpha + \alpha^{-1})\left(\frac{\alpha^2}{12} - \frac{1}{2} + \frac{1}{12\alpha^2}\right) + \frac{2}{3}\left(\alpha\, arctan(\alpha^{-1}) + \frac{arctan(\alpha)}{\alpha}\right) - \frac{7}{12} \end{aligned} \tag{A-8}$$

and $\alpha = w/h$ is the aspect ratio of the rectangle. Because $\ln(e(\alpha)) = \ln(e(1/\alpha))$, using the aspect ratio $\alpha = h/w$ will give the same value. Indeed, equation A-8 was written in a way to illustrate this property. Thus, the self inductance is

$$S(w,h,l) = \frac{\mu_o l}{2\pi}\left(\ln\left(\frac{2l}{w+h}\right) + 0.5 - \ln(e(\alpha))\right) . \tag{A-9}$$

Grover also expresses this self inductance as

$$S(w,h,l) = \frac{\mu_o l}{2\pi}\left(\ln\left(\frac{2l}{K(\alpha)(w+h)}\right) - 1\right) , \tag{A-10}$$

where $K(\alpha) = \exp(-1.5 + \ln(e(\alpha)))$. The advantage of this expression is that the function *K(α)* is nearly a constant for all aspect ratios. It has a minimum value of about 0.22313 when $\alpha = 0$ and a maximum value of about 0.22360 when $\alpha = 0.5$. Thus, the self inductance can be approximated by using the mean value of the minimum and the maximum 0.22337 for *K(α)* for any aspect ratio, i.e.,

$$S(w,h,l) \approx \frac{\mu_o l}{2\pi}\left(\ln\left(\frac{2l}{0.22337\,(w+h)}\right) - 1\right) . \tag{A-11}$$

The off diagonal elements of the inductance matrix are the mutual inductances between two different rectangular elements where the centers that are separated by a distance $p=s+w$. Grover also has tables that are used to calculate this mutual inductance, but only where the widths are equal, the heights are equal, and the line joining the centers is either perpendicular or parallel to the sides such as the rails shown in figures 1 and 4 of this report. The geometric mean distance to be used in equation A-5 in this case is

$$\ln(R) = \frac{1}{2w^2h^2} \int_{(-p-w)/2}^{(-p+w)/2} dx \int_{(p-w)/2}^{(p+w)/2} dx' \int_{-h/2}^{h/2} dy \int_{-h/2}^{h/2} dy' \ln\left((x-x')^2 + (y-y')^2\right) . \tag{A-12}$$

Defining $\alpha = w/h$ and $\beta = p/h$, the integrations give

$$\ln(R) = \ln(p) + \ln(k(\alpha,\beta)) , \tag{A-13}$$

where

$$\ln(k(\alpha,\beta)) = -\ln(\beta) - 3/2 + \frac{1}{\alpha^2}\left(g(\beta+\alpha) + g(\beta-\alpha) - 2g(\beta)\right) \tag{A-14}$$

and

$$g(\gamma) = -\frac{\gamma^4 - 6\gamma^2 + 1}{24}\ln(\gamma^2+1) + \frac{\gamma(\gamma^2-1)}{3}\left(\frac{\pi}{2} - \arctan\left(\frac{1}{\gamma}\right)\right) + \frac{\gamma^4}{12}\ln(\gamma) - \frac{7\gamma^2}{24} . \tag{A-15}$$

If the rails have equal width and heights and if the rails had a uniform current distribution, the inductance gradient of a railgun can be calculated by using equation A-13 and equation A-9. When the rails are conducting equal but opposite currents, the inductance of the rails is

$$L = 2(S(w,h,l) - M(w,h,p)) , \tag{A-16}$$

where

$$M(w,h,p) = \frac{\mu_o l}{2\pi}\left(\ln(2l) - \ln(p) - \ln(k(\alpha,\beta) - 1\right). \tag{A-17}$$

With this equation, equation A-9, and equation A-15, the inductance gradient is

$$L' = \frac{\mu_o}{\pi}\left(\frac{1}{\alpha^2}\left(g(\beta+\alpha) + g(\beta-\alpha) - 2g(\beta)\right) - \ln(1+\alpha) - \ln(e(\alpha))\right) , \tag{A-18}$$

where α must be w/h.

The off diagonal elements of the inductance matrix, however, require a more general formula for the mutual inductance, where the elements may be located anywhere and may have different widths and heights as shown in figure A-1. Let element "*a*" have a width w_a and a height h_a and

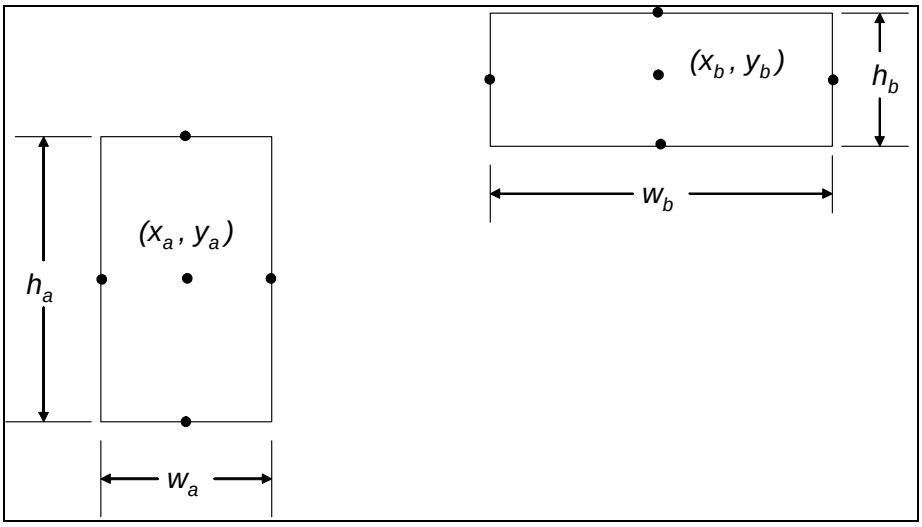

Figure A-1. Two elements with the locations of filaments (●) used for the mutual inductance in equation A-17.

have its center located at (x_a,y_a). Let element "*b*" have a width w_b and a height h_b and have its center located at point (x_b, y_b). Instead of performing the integrals in equation A-2 for an analytical formula, these integrals are approximated by expanding the integrand in a Taylor series and then integrating over the two regions of the elements. This procedure gives this mutual inductance as a sum of mutual inductances between filaments, equation A-19, that are located at the dots in figure A-3.

$$m(x, y, x', y') = \frac{\mu_o}{2\pi}\left(\ln\left(\frac{2l}{\sqrt{(x-x')^2 + (y-y')^2}} \right) - 1 \right) . \qquad \text{(A-19)}$$

In equation A-19, the location of one filament is (x,y) and the location of the other filament is (x',y'). Both filaments have the same length l. Thus, the approximate mutual inductance between the elements in terms of equation A-19 is

$$\begin{aligned} 6M(x_a, y_a, w_a, h_a, x_b, y_b, w_b, h_b) = {} & m(x_a, y_a, x_b + w_b/2, y_b) + m(x_a, y_a, x_b, y_b + h_b/2) \\ & + m(x_a, y_a, x_b - w_b/2, y_b) + m(x_a, y_a, x_b, y_b - h_b/2) \\ & + m(x_a + w_a/2, y_a, x_b, y_b) + m(x_a, y_a + h_a/2, x_b, y_b) \\ & + m(x_a - w_a/2, y_a, x_b, y_b) + m(x_a, y_a - h_a/2, x_b, y_b) \\ & - 2m(x_a, y_a, x_b, y_b). \end{aligned} \qquad \text{(A-20)}$$

This approximation was checked with equation A-13 by setting $w_a = w_b$, $h_a = h_b$, $y_a = y_b$, and varying the distance between the centers, $x_b - x_a$. The difference in the mutual inductances is well within one percent when the elements are bordering each other. The two equations give nearly identical results when the distance between the centers is on the order of two to three times the width or height.

When there is cylindrical symmetry and the conductors are divided up into concentric rings with square cross sections, the inductance matrix has the self-inductance of the rings on the diagonal and the mutual inductance on the off diagonal. According to Grover[1], the self inductance of a ring with a square cross section is

$$L = \mu_o a N^2 \left(\frac{1}{2}\left(1+\frac{1}{6}\left(\frac{c}{2a}\right)^2\right)\ln\left(\frac{8}{\left(\frac{c}{2a}\right)^2}\right) - 0.84834 + 0.2041\left(\frac{c}{2a}\right)^2 \right), \qquad \text{(A-21)}$$

where c is the width or height of the square and a is the distance from the center of the ring to the center of the square. N is the number of turns, but there is only one turn $N = 1$ for the rings. The mutual inductance between two rings is approximated in the same procedure for estimating the mutual inductance between two rectangular bars, but by starting with the mutual inductance between two filamentary loops:

$$M = \frac{\mu_o \sqrt{(r+r')^2 + \Delta z^2}}{2}\left((2-m)K(m) - 2E(m)\right), \qquad \text{(A-22)}$$

where r and r' are the radii of the filamentary loops and Δz is the distance between their centers,

$$m = \frac{4rr'}{(r+r')^2 + \Delta z^2}, \qquad \text{(A-23)}$$

$$K(m) = \int_0^{\pi/2} (1 - m\sin^2\theta)^{-1/2}\, d\theta, \qquad \text{(A-24)}$$

and

$$E(m) = \int_0^{\pi/2} (1 - m\sin^2\theta)^{1/2}\, d\theta. \qquad \text{(A-25)}$$

K(m) and *E(m)* are the complete elliptic integrals of the first and second kind, respectively. Using this formula for the filamentary loops, the mutual inductance between two rings that have rectangular cross sections. Suppose that the rectangles in figure A-1 are the cross sections of two rings where the x-coordinate would be the z-coordinate for the ring and the y-coordinate would be the r-coordinate. Thus, the mutual inductance of the two rings is then approximated by equation A-20. The resistance for the ring is $R = 2\pi a/\sigma c^2$, where c is the width or height of the square and a is the distance from the center of the ring to the center of the square, same as equation A-21. σ is the conductivity of the ring.

NO. OF
COPIES ORGANIZATION

1 (PDF only) DEFENSE TECHNICAL INFORMATION CTR
DTIC OCA
8725 JOHN J KINGMAN RD
STE 0944
FORT BELVOIR VA 22060-6218

1 DIRECTOR
US ARMY RESEARCH LAB
IMNE ALC HRR
2800 POWDER MILL RD
ADELPHI MD 20783-1197

1 DIRECTOR
US ARMY RESEARCH LAB
RDRL CIM L
2800 POWDER MILL RD
ADELPHI MD 20783-1197

1 DIRECTOR
US ARMY RESEARCH LAB
RDRL CIM P
2800 POWDER MILL RD
ADELPHI MD 20783-1197

1 DIRECTOR
US ARMY RESEARCH LAB
RDRL D
2800 POWDER MILL RD
ADELPHI MD 20783-1197

ABERDEEN PROVING GROUND

1 DIR USARL
RDRL CIM G (BLDG 4600)

NO. OF
COPIES ORGANIZATION

ABERDEEN PROVING GROUND

20 DIR USARL
RDRL WMP A
P BERNING
J FLENIKEN
C HUMMER (5 CPS)
T KOTTKE
M MCNEIR
A PORWITZKY
J POWELL
B RINGERS
G THOMSON
G UHLIG
T VALENZUELA
RDRL WMP D
A BARD
B DONEY
M KEELE
G VUNNI
RDRL WMP E
P BARTKOWSKI

INTENTIONALLY LEFT BLANK.